# COMPOSITION VARIATIONS IN THE SOLAR CORONA AND SOLAR WIND

J. C. RAYMOND
*Harvard-Smithsonian Center for Astrophysics*

**Abstract.** Order of magnitude variations in relative elemental abundances are observed in the solar corona and solar wind. The instruments aboard SOHO make it possible to explore these variations in detail to determine whether they arise near the solar surface or higher in the corona. A substantial enhancement of low First Ionization Potential (FIP) elements relative to high FIP elements is often seen in both the corona and the solar wind, and that must arise in the chromosphere. Several theoretical models have been put forward to account for the FIP effect, but as yet even the basic physical mechanism responsible remains an open question. Evidence for gravitational settling is also found at larger heights in quiescent streamers. The question is why the heavier elements don't settle out completely.

**Key words:** corona, solar wind, composition

## 1. Introduction

Abundance variations are frequently observed in the solar wind and the solar corona. Factor of 3 changes in conveniently measured abundance ratios, such as O:Mg and Ne:Mg are common, and factor of 10 departures from photospheric abundance are sometimes observed. We care about these anomalies because

1. Abundance variations provide a means for connecting features in the corona with structures in the solar wind.
2. Knowledge of the composition is *required* to correctly apply many diagnostics, such as X-ray band ratios used to derive electron temperatures (Li *et al.* 1998).
3. The radiative cooling rate enters into models used to understand coronal heating, and it depends on elemental abundances.
4. Composition is a unique signature of the connection between the chromosphere and corona and of the physical processes involved in heating and accelerating the solar corona and solar wind. Unfortunately, like some of the viewgraphs on which this review is based, that signature is difficult to read.

The predominant pattern observed in both the solar wind and in the corona is the FIP effect—the enhancement of elements whose neutral atom has an ionization potential below 10 eV (low-FIP) relative to the high-FIP elements. The 10 eV dividing line is likely to be associated with the energy of a Ly$\alpha$ photon. The abundant low-FIP elements are Na, Si, Al, Ca, Fe and Ni, while He, N, O, Ne and Ar are high-FIP. The intermediate FIP elements C and S show intermediate enhancement. The FIP enhancement is typically a factor of 3–4 in the slow solar wind and less than 2 in the fast wind. Most observations give relative rather than absolute abundance determinations, so a longstanding question is whether the low-FIP elements are enhanced or the high-FIP elements are depleted. The element

*Space Science Reviews* **87**: 55–66, 1999.

fractionation must occur where the low-FIP elements are ionized and the high-FIP elements are neutral. SOHO measurements show the FIP effect and its variation among different coronal and solar wind structures. They also reveal an abundance anomaly interpreted as gravitational settling of the heavy elements in quiescent structures at high altitudes.

A number of comprehensive reviews of both observations and theoretical explanations of coronal and solar wind composition are available (Meyer 1985; Saba 1995; Feldman 1992; Henoux 1995). A volume of *Space Science Reviews* edited by R. von Steiger presenting abundance results from a recent ISSI workshop is due to appear shortly. This paper summarizes the measurements, concentrating on recent results from SOHO and Ulysses. It discusses the analysis and the uncertainties involved, particularly for absolute abundance determinations. It briefly summarizes the currently available theoretical models.

## 2. Measurements

### 2.1. Photospheric Composition

While it is interesting to observe variations in the coronal or solar wind composition from point to point and time to time for their own sake, any interpretation of the cause of the variations will eventually require knowledge of how the fractionation mechanism affects the composition, i.e., how the coronal and solar wind compositions compare with the photospheric values. Photospheric abundances for most elements are determined from absorption line profiles and the assumption of Local Thermodynamic Equilibrium. Thus they are sensitive primarily to the photospheric temperature structure and to the oscillator strengths of the transitions observed. Errors may arise as a result of averaging over the fluctuations in photospheric temperature associated with granulation. This is most likely to affect elements for which only a minority ionization stage can be observed (see the discussion of the Li abundance by Kurucz 1995) or elements for which only transitions among highly excited states can be observed in the optical.

Abundance errors will also result from errors in the oscillator strengths. While the oscillator strengths are among the easier atomic parameters to compute, and they are more accurately known than collisional excitation cross sections, ionization rates or recombination rates, there have occasionally been major recalibrations of the abundance scale due to changes in the oscillator strengths of complex elements such as iron. The oscillator strengths are likely to be reliable to about the 20% level for complicated species and better for simple ions. Some elements are not easily observed at optical wavelengths, and their abundances are obtained from meteorite composition scaled to elements that can be observed in the solar photosphere.

Anders and Grevesse (1989) presented a comprehensive abundance analysis. A recent study by Boyarchuk *et al.* (1998) confirmed the Anders and Grevesse values

for the preferred atmospheric model, but found offsets of order 0.1 the logarithm for abundances based on other model atmospheres.

Feldman (1992) presents a fairly recent compilation of photospheric abundances, and we will use that set of abundances for reference. Most of these values are from Anders and Grevesse (1989) with a few updated values. The Ne abundance is taken from local galactic and flare measurements. It is unfortunate that the Ne abundance is especially difficult to determine, because neon is frequently used as the indicator for high-FIP abundances.

### 2.2. Solar Wind Abundances

Variations in the ratio of He to H in the solar wind have long been known, and as instrumental capabilities improved other elements were seen to vary. The He to H ratio is fairly constant at about 0.05 in the fast solar wind, or about half solar (e.g., von Steiger *et al.* 1995). In the slow wind, the helium abundance is even lower, and it varies on short time scales. Especially low helium abundances are associated with the interplanetary current sheet. During Coronal Mass Ejections (CMEs), the helium abundance can reach 30% and enhanced heavy element abundances are sometimes seen (Galvin 1997). CELIAS measurements of abundances in the 6 January 1997 CME show a systematic enhancement of heavy elements in the CME and erupted filament material, with Fe/O about an order of magnitude above the photospheric value with no FIP signature (Wurz *et al.* 1998), though this result may depend upon the charge state assumed in analyzing the data.

The FIP effect has been observed under a wide range of solar wind conditions, usually based on relative abundances such as the Mg/O or Fe/O ratios. Absolute abundance determinations are more difficult due to the large dynamic range needed to compare proton fluxes with fluxes of trace elements. The Mg/O enrichment is typically a factor of 3.3 in the slow solar wind, and less than half as great in the fast wind (Geiss *et al.* 1995). The enhancement is quite constant in the fast wind, and strongly variable in the slow wind. Besides the clear correlation with solar wind speed, the Mg/O ratio is correlated with the freeze-in temperatures derived from the ionization state of the wind.

Measurements were made of the Fe/O ratio with the CELIAS experiment on SOHO while solar minimum conditions prevailed (Aellig *et al.* 1998). The average ratio of $0.11 \pm 0.03$ indicates a factor of 3 FIP bias, and as with the Ulysses measurements, the enhancement ranges from about 0.12 at the lowest speeds to 0.06 when the speed exceeds 500 km/s (Ipavich *et al.* 1992; Geiss *et al.* 1995). The high time resolution of the CELIAS instrument shows strong variability on a time scale of hours. The anticorrelation of FIP bias with wind speed and correlation with freeze-in temperature hold in a general way at the shorter time scales, but Aellig *et al.* present a remarkable example of a 6 hour offset between a sharp jump in the Fe/O ratio and the corresponding jump in the other variables.

Abundance anomalies are also observed in Solar Energetic Particles (Reames 1990, 1992). A mass bias attributed to the $Q/A$ dependence of the acceleration process is superimposed on the FIP bias (Meyer 1985). The strength of the FIP effect varies from one event to another. A strong FIP bias is taken to mean that the particles were accelerated by CME-driven shocks in the coronal regions associated with the slow solar wind, while a weaker FIP bias could mean that they arise in the flare or in shock acceleration in fast solar wind regions. The abundance of $^3$He can be enhanced by orders of magnitude in events associated with impulsive solar flares, and these events also show enhancements of heavy elements.

## 2.3. Coronal Abundances

### 2.3.1. *X-ray Observations*

There have been indications of abundance variations in the solar corona for many years. X-ray observations of solar flares suggested changes in the Ca abundance from line-to-continuum ratios (Sylwester *et al.* 1984). As this method compares the emission of the dominant He-like ion with bremsstrahlung continuum produced by electrons at similar energies, it is relatively insensitive to uncertainties in atomic rates and to uncertainty in the instrumental calibration. Because the bremsstrahlung is largely produced by collisions with protons, it yields an absolute abundance measurement. Fludra and Schmelz (1995) concluded that low-FIP elements were enhanced by factors of 1.5–2, while oxygen was depleted by a factor of 4 from one set of observations. Sylwester *et al.* (1998) derived an average calcium abundance of $5.8 \times 10^{-6}$ from over 100 flares, or about twice the photospheric value. The abundances are likely to depend on the fraction of flare plasma provided by evaporation of chromospheric material.

Another approach to solar flare abundances is a comparison of the Fe XXV emission line flux produced in the flare to the fluorescent Fe K$\alpha$ emission produced when X-rays from the flare ionize material at the solar surface (Phillips *et al.* 1994). This method compares the coronal iron abundance to the abundance in the photosphere, again cancelling out instrumental calibration uncertainties. This method has not been applied to a large number of flares, but it seems to show photospheric iron abundances in the flare plasma.

The most widely used approach to deriving coronal abundances from X-ray spectra is to pair lines of different elements that are formed at the same temperature to obtain the relative abundances of those elements. Ne IX and Fe XVII are particularly convenient in that these are the dominant ions of their respective elements over a large, and largely overlapping, temperature range, the lines are strong and close together in wavelength, and they represent a high- and a low-FIP element (Schmelz *et al.* 1996; Phillips *et al.* 1997). The results have been somewhat controversial due to differences in the Fe XVII ionization balance calculations used and due to disagreement about the importance of resonance scattering in the Fe XVII 15.01 Å line.

In general, X-ray abundance studies employ strong emission lines of relatively simple ions. The collisional excitation rates for these transitions should be accurate to about 20% or better. Phillips and Feldman (1997) have investigated the analysis of abundances, ionization state and temperature based on S, Ca and Fe K line measurements from YOHKOH. They find consistency at the 50% level.

### 2.3.2. *UV Observations*

An extensive series of papers has explored the FIP effect in a wide variety of coronal structures based on the relative intensities of the Mg VI and Ne VI multiplets near 400 Å (e.g., Widing and Feldman 1989; Sheeley 1996). The lines are formed at the same temperature in coronal equilibrium (about $2 \times 10^5$ K), and their wavelengths are so close that instrumental sensitivity can be safely assumed to be the same for the two sets of lines. Order of magnitude variations in the line ratios, and by inference the relative abundances of Mg and Ne, were reported. Though there was initially skepticism about abundances derived from a single pair of ions, density effects and departures from ionization equilibrium seem unable to account for the large line ratio variations observed (Jordan *et al.* 1997). In general unipolar field regions were FIP-enhanced, while small bipolar regions were not. It seems plausible that impulsive events lift chromospheric material more or less unchanged, while fractionation over a longer time scale enhances the low-FIP elements in large scale features. Spicer *et al.* (1998) used Mg VI and Ne VI to investigate the FIP effect in prominences. They found intermediate FIP enhancements between the photospheric and coronal abundance sets.

Young and Mason (1997) have extended the Ne:Mg study by observing a set of two ions of Ne and three ions of Mg with the CDS instrument on SOHO, along with an O IV density-sensitive line ratio to help compensate for density dependence of the Ne and Mg line intensities. The range of ions eliminates the possibility that a shift in ionization state might give a spurious abundance, and it provides consistency checks on the atomic rates. Young and Mason found that the Ne:Mg ratio within the active region they observed depends upon the type of the feature observed. The "spike" feature which they identified as a larger, older magnetic loop showed an Mg/Ne enhancement as large as a factor of 9, while the apparently younger, newly emerged loops showed a photospheric abundance ratio.

Coronal abundance studies have also been performed with the SUMER spectrometer on SOHO. Doschek *et al.* (1998) compared the FIP-sensitive ratios of silicon and magnesium to neon in coronal holes and the quiet Sun. They observed lines from two ions of Ne, four ions of Mg and two ions of Si to avoid ionization balance uncertainties, but atomic rate uncertainties and radiometric calibration uncertainties limited the analysis to a factor of 2 accuracy, close to the strength of the effect being sought. Doschek *et al.* showed that the apparent factor of 2 FIP bias in coronal hole interplume regions is probably real. No difference was observed between coronal hole and quiet Sun abundances. The ions observed are formed over the $5 \times 10^5$ to $1.5 \times 10^6$ K range, so the abundances pertain to the upper transition

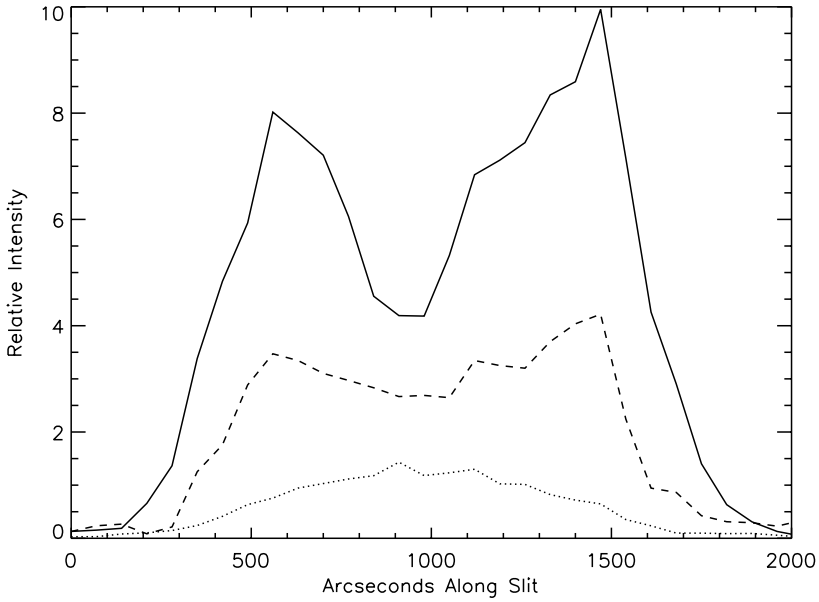


*Figure 1.* Relative intensities of O VI $\lambda$1032 (solid line), Si XII $\lambda$499 (dashed line) and Ly $\beta$ (dotted line) along the UVCS spectrograph slit for the equatorial streamer observed in July 1996. While Ly $\beta$ peaks near the center of the streamer, the other lines peak near the streamer edges.

region and corona. On the other hand, a set of SUMER observations 22″ above the limb in a coronal hole analyzed by Feldman *et al.* (1998) showed no FIP effect at all.

At greater heights, the UVCS instrument on SOHO has obtained abundances in coronal streamers. Because the UVCS spectral range includes several of the H I Lyman lines, and because the coronagraph effectively rejects stray light from the solar disk (Kohl *et al.* 1996), it is possible to obtain absolute abundances. Raymond *et al.* (1997) analyzed an equatorial streamer observed in July 1996, while the sun was still at solar minimum. At 1.5 $R_\odot$ the line intensities show the surprising behavior shown in Figure 1. While the H I Lyman line intensities peak at the streamer center (along with the white light brightness, as reported by Gibson *et al.* 1998 for the same streamer one solar rotation later), the line intensities of the other elements peak at the edges of the streamer. Both high and low ionization states (e.g., Si XII and O VI are shown in the figure) behave in this manner, so it is not a result of variation in ionization state. Doppler dimming studies show that the outflow speed is small, and variation in the relative importance of collisional excitation and radiative scattering cannot account for the different behavior. Thus substantially different abundances in the center and legs of the streamer are required (Noci *et al.* 1997).

Table I.
Elemental Abundance Estimates

| Element | Photosphere | Corona | Center | Leg | Active |
|---|---|---|---|---|---|
| H | 12.00 | 12.00 | 12.00 | 12.00 | 12.00 |
| He | 10.99 | 11.00 | $\leq$10.7 | $\leq$11.0 | $\leq$11.1 |
| N | 8.00 | 7.59 | $\leq$7.40 | $\leq$7.60 | $\leq$7.60 |
| O | 8.93 | 8.39 | 7.80 | 8.40 | 8.50 |
| Ne | 8.11 | 7.54 | $\leq$8.4 | $\leq$8.6 | $\leq$8.6 |
| Mg | 7.58 | 7.57 | 7.1 | 7.4 | 7.7 |
| Al | 6.47 | 6.44 | 5.7 | 5.9 | 6.3 |
| Si | 7.55 | 7.59 | 6.7 | 7.1 | 7.5 |
| S | 7.21 | 6.94 | 6.2 | 6.6 | 6.6 |
| Ar | 6.65 | 6.33 | — | 6.1 | 6.2 |
| Ca | 6.36 | 6.47 | — | 6.1 | 6.2 |
| Fe | 7.51 | 7.57 | 7.0 | 7.5 | 7.4 |
| Ni | 6.25 | 6.33 | — | — | 6.3 |

Analysis of the line intensities from the UVCS spectra yields the abundances listed in Table I. The photospheric and coronal abundances from Feldman's (1992) compilation are given for comparison. Spectra were extracted for the $500''$ near the streamer center where the O VI intensity is lowest ("Center"), for the brighter of the two O VI peaks ("Leg") and for a complex set of streamers on the other limb of the Sun above a pair of active regions to the north and south of the solar equator ("Active"). It is apparent from the table that a factor of 3 FIP bias is present in all three spectra. What is surprising is the sense of the FIP bias. Instead of an enhancement of the low-FIP elements with respect to the photosphere, the high-FIP elements are depleted by a factor of 3 in the Leg and Active spectra, and in the streamer core the low-FIP elements are down by a factor of 3 and the high-FIP elements are depleted by a factor of 10, a more extreme value than is generally encountered even in the slow solar wind. A plausible explanation for these observations is that the FIP bias is imposed at the chromospheric level for both streamer legs and streamer core. Because the streamer is so quiescent (it remained largely unchanged for several solar rotations), gravitational settling reduces the abundances of the heavier elements in the streamer core. This is completely plausible if the streamer core is considered to be an arcade of closed magnetic loops. If the streamer core is open (Noci *et al.* 1997), material may be flowing out through the core and the low abundance in the streamer center may require a change in the drag due to variation of the ion-ion collision rate with changing density.

SUMER observations in the core of an equatorial streamer reconcile the depletions derived from UVCS at 1.5 $R_\odot$ with the view that in general high-FIP elements are at normal abundance and low-FIP elements are enhanced (Feldman *et al.* 1998).

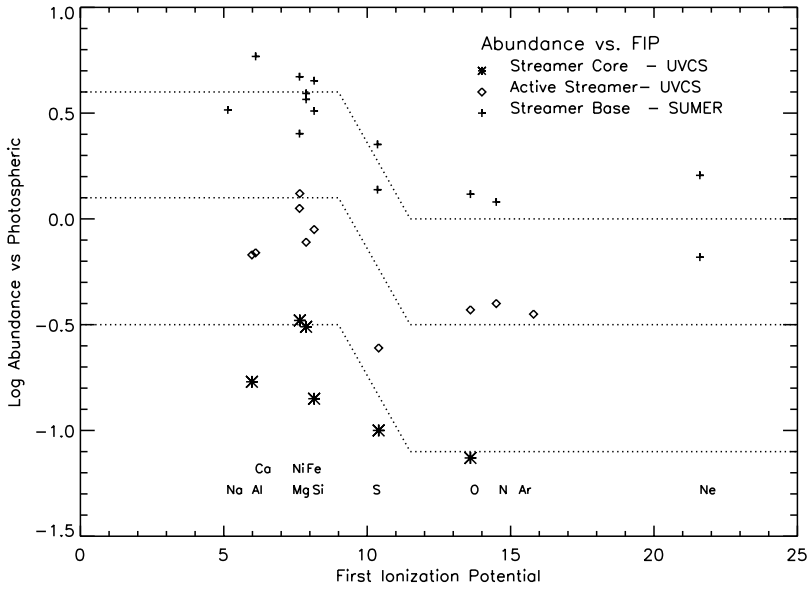


*Figure 2.* Elemental abundances plotted against First Ionization Potential from UVCS data (Streamer Core and Active Streamer; Raymond *et al.* 1997) and SUMER (Streamer Base; Feldman *et al.* 1998). The UVCS data were obtained at 1.5 $R_\odot$ and the SUMER data pertain to heights below 1.03 $R_\odot$. For comparison with the three sets of data, the dotted lines show for a FIP bias of 4 matched to the high-FIP elements for each data set.

Close to the surface, the SUMER spectra showed high-FIP abundances close to photospheric and low-FIP elements enhanced by a factor of 4. Emission lines of different elements declined at different rates with height above the limb, however, with Fe lines dropping more quickly than lines of other elements. This confirms the gravitational settling interpretation of the UVCS data. Figure 2 shows the UVCS abundances obtained for a streamer core and an active region streamer, along with the SUMER abundances for the base of an equatorial streamer.

Few abundance measurements are available so far for CMEs near the Sun. UVCS observations of prominence ejecta in the 11 December 1997 event include lines of Si III, C III, N V, S V] and O VI (Ciaravella *et al.* 1998). Most of the observed lines arise from high-FIP ions, making study of the FIP effect difficult, but the Si/C and S/O ratios appear consistent with photospheric values.

The uncertainties in the abundances derived from UV spectra of the corona include uncertainties in (1) collisional excitation rates, (2) radiometric calibration, (3) the separation of stray light and scattering contributions to the line intensities, and (4) the ionization state of the plasma. Uncertainties in excitation rates of the lines generally used should be in the 10%–30% range. Both SUMER and UVCS were carefully calibrated in the laboratory and their radiometric calibration has been

monitored with observations of stars above 912 Å. Thus the uncertainties should be no more than 15% at long wavelengths. At shorter wavelengths it is less clear what uncertainty to assign, but cross calibration of the UVCS instruments will provide an estimate. Stray light levels should be quite small for SUMER spectra close to the limb and for the UVCS spectra discussed above. For SUMER spectra at larger heights and for UVCS offset pointings (below 1.4 $R_\odot$) corrections must be made based on the apparent intensities of lines from the chromosphere. Separation of collisional and radiative scattering contributions of the H I Lyman lines and the O VI doublet is straightforward. For instance, the O VI doublet intensity ratio is 2:1 for the collisional component and 4:1 for disk photons scattered by O VI ions in the corona (provided the outflow speed is small). Some uncertainty may arise from the details of the chromospheric Ly$\alpha$ and Ly$\beta$ profiles and the relative radiometric calibration at these wavelengths. Perhaps the largest worry is the ionization state of the plasma, as the abundances shown in Figure 2 are derived from one or two ions of each element. While all three data sets shown indicated remarkably isothermal gas along the line of sight, it is likely that ionization balance uncertainties dominate the error. The scatter in abundances at a single FIP for a given data set in Figure 2 could be real (for instance First Ionization Time rather First Ionization Potential would shift points along the $x$ axis, and mass segregation could shift some elements relative to others in the $y$ direction), but discrepancies such as different abundances of an element derived for different ions suggest that this is the current level of uncertainty in the atomic rates and intensity measurements.

## 3. Theoretical Models

A number of theories have been put forward to explain the FIP effect. All these models rely upon the differing behavior of ions and neutrals in the part of the chromosphere where low-FIP elements are ionized and high-FIP elements are neutral. Some models are based purely on diffusion in a region of strong gradients in temperature, density and ionization state, while other models employ electric or magnetic fields to separate ions from neutrals.

The diffusion models generally treat the heavy elements as test particles in a static or rising hydrogen plasma. Early models produced very strong abundance anomalies (Shine, Gerola and Linsky 1975; Roussel-Dupre 1981). Recent models impose flows of a few hundred meters per second in the chromosphere and produce stronger FIP enhancements in slower flows, reminiscent of the difference between fast and slow solar wind (Peter 1996, 1998) or assume that transient heating evaporates chromospheric material (Wang 1996). In these models the First Ionization Time, rather than First Ionization Potential, is the crucial parameter, in harmony with the measured abundance patterns. A potential difficulty with such steady-flow models is that flux conservation should force the coronal abundances to be the same as those at the lower boundary (McKenzie, Sukhorukova and Axford 1998).

If the diffusion zone is at the bottom of a closed magnetic loop, the FIP bias may increase over the course of time (Zurbuchen *et al.* 1998; Schwadron, Fisk and Zurbuchen 1999). This picture fits in with the observed tendency for the FIP effect to be stronger in older magnetic structures (e.g., Young and Mason 1997). The FIP-enhanced material enters the slow solar wind when reconnection opens the magnetic loops. Thus Schwadron, Fisk and Zurbuchen (1999) propose that wave heating of the ions gives low FIP elements larger scale heights, and that material trapped in magnetic loops develops a FIP bias on a gravitational settling time scale of order a day.

An example of a model based on magnetic separation is the von Steiger and Geiss (1989) model, in which material flows up along a magnetic flux tube. Ions are closely confined by the magnetic field, but neutrals diffuse across field lines and fall out of the flow. The angle of the flux tube from vertical is an important parameter for the strength of the FIP enhancement. Vauclair and Meyer (1985) studied FIP fractionation in a model in which predominantly horizontal magnetic field rises through the chromosphere, lifting ions more efficiently and leaving some neutrals behind. Henoux and Somov (1992) present a model in which twisting of a vertical, diverging flux tube produces vertical currents that lift the ions. A promising model has recently been presented by Arge and Mullan (1998). They use a 2D two-fluid MHD numerical simulation of a magnetic interaction region—a region where opposing magnetic fields are pressed together as in magnetic reconnection models, but without the rapid reconnection and heating sought in flare models. If the magnetic interaction occurs in the chromosphere, it can concentrate ions (low FIP elements) in the field reversal region, and this material could be subsequently ejected by magnetic forces or thermal pressure.

At present it is difficult to choose among the theoretical models for the FIP effect, or even to be certain that one among them captures all the dominant physical processes. The common theme of the loss of efficient collisional coupling in a region of partial ionization must be correct, and all the models can produce a reasonably strong FIP effect. However, all the models have one or more free parameters that are adjusted to match the observed enhancements. Some potential difficulties that FIP effect models must address include

1. Self-consistent models show that protons diffuse downward on average in a static chromosphere-transition region (Fontenla, Avrett and Loeser 1990); this would drive the FIP bias in the wrong direction.
2. The steady chromosphere assumed in many models may not exist, and shocks in a cooler atmosphere provide the UV emission previously attributed to the upper chromosphere (Wikstol *et al.* 1997).
3. The mass circulation associated with spicules is 100 times larger than the net outflows assumed in the diffusion models (Athay 1976).
4. Little is known about the actual magnetic structure and dynamics at small scales in the chromosphere.

The theoretical picture of gravitational settling high in the corona is also unsettling. This may be a result of the smaller number of models put forward so far. The gravitational settling time for streamer material at 1.5 $R_\odot$ is about a day, and the thermal scale height for the heavier elements is so small that species such as iron ought to be depleted by orders of magnitude. Thus either there is a mechanism that mixes fresh material into the streamer with a time scale of order a few days, or there is non-thermal support available for the ions. It is easy to imagine that material flows along magnetic flux tubes, or that reconnection mixes material into the streamer core from along its edges. However, a natural mechanism for supporting the ions in a static or slowly rising flow is readily available, in that non-thermal line widths of order 30 km/s are typical of the low corona (e.g., Mariska *et al.* 1979). At larger heights, lines such as O VI and Mg X reach velocity widths comparable to the widths of the Lyman lines by heights of 4 or 5 $R_\odot$ in streamers (Kohl *et al.* 1997). Lenz, Lou and Rosner (1998) have constructed models of closed magnetic loops including diffusion and a self-consistent treatment of the electric field. They find that elements of differing mass settle in a manner consistent with the SOHO observations for loops of order $10^9$ cm in length, but the abundances of heavy elements are far too small for $10^{10}$ cm loops compared with SOHO observations. Models incorporating wave-particle interactions, constrained by the observed line widths, are badly needed, along the lines of the models being developed for coronal holes (Cranmer *et al.* 1999). More detailed observations will be needed to test the model, and in particular to examine the physics of wave-particle interaction assumed in these calculations and in models of the fast solar wind. As pointed out by Zurbuchen *et al.* (1998) and Schwadron, Fisk and Zurbuchen (1999) the FIP bias and gravitational settling may be intertwined.

This work was supported by NASA Grant NAG5-3192 to the Smithsonian Astrophysical Observatory. It has benefited from useful comments by T. Zurbuchen, A. van Ballegooijen and R. Frazin.

## References

Aellig, M. R., Hefti, S., Grünwaldt, H., Bochsler, P., Wurz, P., Ipavich, F. M., and Hovestadt, D.: 1998, *JGR*, submitted.

Anders, E., and Grevesse, N.: 1989, *N. Geochim. Cosmochim. Acta*, **53**, 197.

Arge, C. N., and Mullan, D. J.: 1998, *Solar Physics*, **182**, 293.

Athay, R. G.: 1976, in *The Solar Chromosphere and Corona: Quiet Sun*, ed. C. J. Macris (Dordrecht: Reidel), p. 36.

Boyarchuk, A. A., Antipova, L. I., Boyarchuk, M. E., and Savanov, I. S.: 1998, *Astronomy Reports*, **42**, 517.

Ciaravella, A., *et al.*: 1998, in preparation.

Cranmer, S. R., Field, G. B., and Kohl, J. L.: 1999, this volume.

Doschek, G. A., Laming, J. M., Feldman, U., Wilhelm, K., Lemaire, P., Schüle, U., and Hassler, D. M.: 1998, *ApJ*, **504**, 573.

Feldman, U.: 1992, *Phys. Script.*, **46**, 202.

Feldman, U., Schüle, E., Widing, K. G., and Laming, J. M.: 1998, *ApJ*, **505**, 999.

Fludra, A., and Schmelz, J. T.: 1995, *ApJ*, **227**, 936.
Fontenla, J. M., Avrett, E. A., and Loeser, R.: 1990, *ApJ*, **355**, 700.
Galvin, A. B.: 1997, in *Coronal Mass Ejections*, N. Crooker, J. A. Joselyn and J. Feynmann, eds. (Washington: AGU), p. 253.
Geiss, J. *et al.*: 1995, *Science*, **268**, 1033.
Gibson, S. E., Fludra, A., Bagenal, F., Biesecker, D., Del Zanna, G., and Bromage, B.: 1998, preprint.
Henoux, J. C.: 1995, *Adv. Sp. Res.*, **15**, No. 7, 23.
Henoux, J. C., and Somov, B. V.: 1992, in Proceedings of the First SOHO Workshop, ESA SP-348, p. 325.
Ipavich, F. M., Galvin, A. B., Geiss, J., Ogilvie, K. W., and Gliem, F.: 1992, in *Solar Wind Seven, COSPAR Colloquium Series, 3.*, E. Marsch and R. Schwenn, eds., p. 369.
Jordan, C., Doschek, G. A., Drake, J. J., Galvin, A., and Raymond, J. C.: 1997, *Tenth Cambridge Workshop on Cool Stars, Stellar Systems and the Sun*, R. Donahue and J. Bookbinder, eds., p. 91.
Kohl, J. L., *et al.*: 1996, *Solar Physics*, **162**, 313.
Kohl, J. L., *et al.*: 1997, *Solar Physics*, **175**, 613.
Kurucz, R. L.: 1995, *ApJ*, **452**, 102.
Lenz, D. D., Lou, Y.-Q., and Rosner, R.: 1998, *ApJ*, **504**, 1020.
Li, J., Raymond, J. C., Acton, L. W., Kohl, J. L., Romoli, M., Noci, G., and Naletto, G.: 1998, *ApJ*, **506**, 431.
Mariska, J. T., Feldman, U., and Doschek, G. A.: 1979, *A&A*, **73**, 361.
McKenzie, J. F., Sukhorukova, G. V., and Axford, W. I.: 1998, *A&A*, **332**, 367.
Meyer, J.-P.: 1985, *ApJ Suppl.*, **57**, 173.
Noci, G., *et al.*: 1997, *Adv. Sp. Res.*, **20**, 2219.
Peter, H.: 1996, *A&A*, **312**, L37.
Peter, H.: 1998, *A&A*, **335**, 691.
Phillips, K. J. H., and Feldman, U.: 1997, *ApJ*, **477**, 502.
Phillips, K. J. H., Pike, C. D., Lang, J., Watanabe, T., and Takahashi, M.: 1994, *ApJ*, **435**, 888.
Phillips, K. J. H., Greer, C. J., Bhatia, A. K., Coffey, I. H., Barnsley, R., and Keenan, F. P.: 1997, *A&A*, **324**, 381.
Raymond, J. C., *et al.*: 1997, *Solar Physics*, **175**, 645.
Reames, D. V.: 1990, *ApJ Suppl.*, **73**, 235.
Reames, D. V.: 1992, in *Proceedings of the First SOHO Workshop*, ESA SP-348, p. 315.
Roussel-Dupre, R.: 1981, *ApJ*, **250**, 408.
Saba, J.: 1995, *Adv. Sp. Res.*, **15** no. 7, 13.
Schmelz, J. T., Saba, J. L. R., Ghosh, D., and Strong, K. T.: 1996, *ApJ*, **473**, 519.
Schwadron, N. A., Fisk, L. A., and Zurbuchen, T. H.: 1999, preprint.
Sheeley, N. R., Jr., *et al.*: 1997, *ApJ*, **484**, 472.
Shine, R., Gerola, H., and Linsky, J. L.: 1975, *ApJL*, **202**, 101.
Spicer, D. S., Feldman, U., Widing, K. G., and Rilee, M.: 1998, *ApJ*, **494**, 450.
Sylwester, J., Lemen, J. R., and Mewe, R.: 1984, *Nature*, **310**, 665.
Sylwester, J., Lemen, J. R., Bentley, R. D., Fludra, A., and Zolcinski, M.-C.: 1998, *ApJ*, **501**, 397.
Vauclair, S., and Meyer, J.-P.: 1985 in *Proc. 19th Int. Cosmic Ray Conf.*, p. 233.
von Steiger, R., and Geiss, J.: 1989, *A&A*, **225**, 222.
von Steiger, R., Wimmer-Schweingruber, R. F., Geiss, J., and Gloeckler, G.: 1995, *Adv. Sp. Res.*, **15**, 3.
Wang, Y.-M.: 1996, *ApJ*, **464**, L91.
Widing, K. G., and Feldman, U.: 1989, *ApJ*, **334**, 1046.
Wikstol, O., Judge, P. G., and Hansteen, V.: 1997, *ApJ*, **483**, 972.
Wurz, P., *et al.*: 1998, *GRL*, **25**, 2557.
Young, P. R., and Mason, H. E.: 1997, *Solar Physics*, **175**, 523.
Zurbuchen, T. Z., Fisk, L. A., Gloeckler, G., and Schwadron, N.A.: 1998, *Space Science Reviews*, **85**, 397.

*Address for correspondence:* Center for Astrophysics, 60 Garden St., Cambridge, MA 02138